

N70-42726

Continual Variations in the
High Energy X-Ray Flux
from Sco X-1

Walter H.G. Lewin, Jeffrey E. McClintock,
Stanley G. Ryckman, Ian S. Glass
and William B. Smith

CSR-P-70-47

August, 1970

CENTER FOR SPACE RESEARCH
MASSACHUSETTS INSTITUTE OF TECHNOLOGY



**CASE FILE
COPY**

Continual Variations in the
High Energy X-Ray Flux
from Sco X-1

Walter H.G. Lewin, Jeffrey E. McClintock,
Stanley G. Ryckman, Ian S. Glass
and William B. Smith

CSR-P-70-47

August, 1970

Continual Variations in the High Energy
X-Ray Flux from Sco X-1*

Walter H. G. Lewin, Jeffrey E. McClintock,
Stanley G. Ryckman, Ian S. Glass and William B. Smith
Center for Space Research
and
Department of Physics
Massachusetts Institute of Technology

Abstract

On 20 March, 1969, we carried out balloon x-ray observations of Sco X-1 (>18 keV) from Australia. We found the intensity to fluctuate continually between $16^{\text{h}}30^{\text{m}}$ and $21^{\text{h}}30^{\text{m}}$ U.T. Intensity changes of factors of two and three were observed within time intervals of one-half to one hour.

During a balloon flight from Mildura, Australia, on 20 March, 1969, we carried out x-ray observations of and made 19 scans over Sco X-1 between $16^{\text{h}}30^{\text{m}}$ and $21^{\text{h}}30^{\text{m}}$ U.T. Simultaneous optical observations were planned from Siding Spring Observatory; quite unexpectedly, however, the observatory clouded out shortly after the balloon reached altitude.

We used our 358 cm^2 NaI(Tl) scintillator detector surrounded by an anticoincidence jacket of plastic scintillator. The field of view had an angular width of 13° FWHM.

*This work was supported by grants from the U.S. National Aeronautics and Space Administration (22-009-015), the National Science Foundation (GP-9365) and the Office of Naval Research.

During the observations of Sco X-1 the telescope axis was inclined to the zenith at angles from 34° to 17° ; the telescope was rotated continuously in azimuth with an average period of about 8 minutes. The zenith angle of the telescope was changed during the Sco X-1 observations to increase the exposure time. These changes were made in a pre-programmed manner; no commands were given from the ground.

At all times the celestial direction of the detector axis could be determined with an accuracy of 1° from continuously recorded azimuthal orientation data provided by two crossed magnetometers which were calibrated by a sun sensor after sunrise ($\sim 20^{\text{h}}10^{\text{m}}$ U.T.). The atmospheric pressure was measured every thirty seconds by a gauge which we calibrated before the flight under simulated flight conditions and found to be accurate to 0.07 g cm^{-2} in our pressure range (2.5 to 3.5 g cm^{-2}). Radar measurements of the altitude agreed with the altitude calculated from the gauge readings. The energy resolution of the detector (FWHM) was 45% at 25 keV and 37% at 60 keV. Before the flight, we determined the seven channel settings of the pulse-height analyzer over the energy range from 18 to 96 keV to an accuracy of about 2%. We monitored the settings for seven seconds every twenty minutes during the flight by exposing the detector to an Am^{241} source. Each seven second calibration period allowed us to determine the counting rate due to the calibration source to a statistical accuracy of about 5% in the lowest

channel, which was the magnitude of the change that could be caused by a shift in the lowest channel boundary (18 keV) of approximately 0.2 keV.

The background counting rate was calculated by combining data over periods of 400 seconds when the field of view included neither Sco X-1 nor any other obvious high energy x-ray source (see, for sky map on October 15, 1967, Lewin, Clark and Smith, 1968a; a similar sky map from the March 20, 1969, observations will be published shortly). The values thus obtained were used with linear interpolation to calculate the background counting rate at any desired instant of the flight. A correlation between the background counting rate and the azimuthal direction of the instrument was found; the counting rate was highest when the instrument was pointing towards the southeast and lowest when the instrument was pointing toward the northwest. Maximum differences from the average value were +3% and -2%. During the observations of Sco X-1 the azimuth of the source changed by about 130° (see table). We have taken the azimuthal dependency of the background into account although it had an insignificant effect on the results obtained for Sco X-1.

During each scan over Sco X-1 the total intensity of the source was calculated in the same way as described in an earlier paper (Lewin, Clark and Smith, 1968b). In our analysis of the Sco X-1 intensity we have taken into account only the data for which the corresponding collimator response function, f (exposed fraction of the sensitive crystal area), was greater than 0.30. Further, we have included only those

scans over Sco X-1 for which, under the above condition, the effective observation time was greater than 15 seconds.

In the table we give detailed information on these 19 scans. Effective observation times vary from a minimum of 16.5 seconds (scan #8) to a maximum of 126.3 seconds (scan #15). During this scan, quite accidentally, the net result of balloon rotation and the telescope's azimuthal driving mechanism resulted in a very slow scan over Sco X-1. One should note that the effective observation time for a given scan depends not only on the azimuthal rotation of the telescope, but also on the difference between the zenith angles of Sco X-1 and the telescope (see columns 3 and 4 of the table). The Universal Times for the moments that Sco X-1 was closest to the axis of the telescope are given in column two; the zenith angle of the telescope, the zenith angle and azimuth of Sco X-1 are given in columns three, four and five. Effective observation times are given in column six; the atmospheric depth is given in column seven and the atmospheric thickness (line of sight to the source) is given in column eight. The absolute accuracy in the values for the atmospheric thickness is 0.07 g cm^{-2} ; the relative accuracy is about 0.04 g cm^{-2} . The counting rates as presented in columns nine and ten include the combined data from our three lowest energy channels (total range, 18-38 keV). Average background counting rates, as calculated in the manner described above, are given in column nine; each value has a statistical accuracy of about

0.5 counts sec^{-1} . Column ten contains the intensity of Sco X-1 in counts sec^{-1} as measured, with no corrections included for detector response or for absorption due to the Earth's atmosphere.

Figure 1 shows the source intensities (18-38 keV) plotted versus Universal Time. Here the intensities are corrected to an atmospheric thickness of 3.50 g cm^{-2} by factors derived under the working assumption that the primary energy spectrum has the form $F(E) \propto \exp(-E/E_0)$ with $E_0 = 5 \text{ keV}$. This form, representing the high-energy cutoff of a thermal bremsstrahlung spectrum, serves here the purpose of describing a steep primary spectrum over the energy range of our observations. In the last column of the table we give correction factors that reduce the data to an atmospheric thickness of 3.50 g cm^{-2} ; the intensities plotted in figure 1 are products of the intensities listed in the table (column 10) and the corresponding correction factors in column 11.

Figure 1 also shows a calculated value for the intensity in the energy range 18 to 38 keV as derived from our observations (20 to 30 keV) on October 15, 1967 between $03^{\text{h}}10^{\text{m}}$ and $04^{\text{h}}15^{\text{m}}$ U.T. (Lewin, Clark and Smith, 1968b). During this period Sco X-1 was in a quiescent state and its intensity was comparatively steady. The extrapolation (from a 20-30 keV channel to an 18-38 keV channel) was made under the assumption of a primary spectrum of the above form with $E_0 = 5 \text{ keV}$.

Positive identification of x-rays from Sco X-1 could be made in only the first three channels (18-22 keV, 22-29 keV

and 29-38 keV). Plots similar to the one given in figure 1 have been made for each of these three energy channels. However, the statistical significance of the data does not allow a meaningful comparison between the intensity fluctuations in these channels. We have therefore presented in figure 1 only the data of the three lowest energy channels combined.

We corrected the data to zero atmospheric thickness using factors derived under the above working assumption regarding the form of the primary spectrum with $E_0=5$ keV. These factors accounted for the atmospheric attenuation and the detector response as described in detail in a previous publication (Clark, Lewin and Smith, 1968). The results of the combined data from all 19 transits over the source are given in figure 2 together with results from previous balloon, rocket, and satellite observations. The spectrum that we thus find fits that of a thermal bremsstrahlung spectrum with values of $4.5 \text{ keV} < E_0 < 7.0 \text{ keV}$. We also calculated separately two average primary spectra, one using only data from the nine scans during which the highest source intensities were observed, and one using data from the other ten scans. The spectra that we thus find (not shown here) also fit the form of a thermal bremsstrahlung spectrum, with values $4.5 \text{ keV} < E_0 < 7.5 \text{ keV}$. Therefore, although we observed strong intensity changes, we have no evidence for a change in the spectral form.

Intensity curves of appearance similar to that presented here have been reported for the optical range of the spectrum

(Hiltner and Mook, 1968; Westphal, Sandage and Kristian, 1968). In addition, the characteristic variation of the optical intensity inferred by Wilson and Twigg, 1970, from various observers' data is not unlike our result (fig. 1). The magnitude of the intensity changes observed in the optical spectrum, however, is considerably smaller than that observed in the x-ray region of the spectrum.

In summary, we have found that there are periods of continual changes in the x-ray intensity of Sco X-1 in addition to flare-type activity which has previously been reported by Lewin, Clark and Smith, 1968b, and by Hudson, Peterson and Schwartz, 1970. Intensity changes have also been reported by Agrawal et al., 1969.

We thank A. Sandage and O. Eggen for their collaboration in attempts to achieve simultaneous optical observation of Sco X-1. We thank E. Curwood, D. Scott, and the staff of the Balloon Launching Station at Mildura, Australia, for carrying out the flight. We also wish to thank R. Leslie and the Australian Ministry of Supply for their cooperation. We are grateful to the staff of the Meteorology Department in Mildura for their frank cooperation and we thank Bill Wilson of the Office of Naval Research for his helpful suggestions during the field operations.

Figure Captions

Figure 1. X-ray intensities (18-38 keV) from Sco X-1 as observed during 19 scans over the source on March 20, 1969. The intensities (counts $\text{sec}^{-1} 358^{-1} \text{cm}^{-2}$) have been corrected to an atmospheric thickness of 3.50 g cm^{-2} . An intensity in this same energy interval as extrapolated from results obtained from observations when Sco X-1 was steady and quiescent on October 15, 1967 (Lewin, Clark and Smith, 1968b) is also indicated.

Figure 2. Spectral data on Sco X-1 obtained from recent balloon, rocket and satellite observations.

References

- Agrawal, P. C., Biswas, S., Gokhale, G. S., Iyengar, V. S., Kunte, P. K., Manchanda, R. K., and Sreekantan, B. V., *Nature*, 224, 51 (1969).
- Clark, G. W., Lewin, W. H. G. and Smith, W. B., *Ap. J.*, 151, 21 (1968).
- Hiltner, W. A. and Mook, Delo E., *Ap. J.*, 150, 851 (1967).
- Hudson, Hugh S., Peterson, Laurence E. and Schwartz, Daniel A., *Ap. J. (Letters)*, 159, L51 (1970).
- Lewin, W. H. G., Clark, G. W. and Smith, W. B., *Ap. J. (Letters)*, 152, L49 (1968a).
- Lewin, W. H. G., Clark, G. W. and Smith, W. B., *Ap. J. (Letters)*, 152, L55 (1968b).
- Westphal, J. A., Sandage, Allen, and Kristian, Jerome, *Ap. J.*, 154, 139 (1968).
- Wilson, Robert E. and Twigg, Laurence W., *Nature*, 226, 734 (1970).

Table

Scan	U.T. March 20 1969	Zenith Angle Telesc. (degs)	Zenith Angle Sco X-1 (degs)	Azimuth Sco X-1 (degs)	Eff. Obs. Time f>0.3 (sec)	Atm. Depth (g cm ⁻²)	Atm. Thickness (g cm ⁻²)	Backgr. Rate (sec ⁻¹) 18 - 38 keV	Intensity* Above Backgr. (sec ⁻¹)	Corr. Fact. to 3.50 g cm ⁻²
Column	2	3	4	5	6	7	8	9	10	11
	16 ^h 42.1 ^m	In-flight energy calibration								
1	16 56.1	29.1	33.0	61.3	30.4	3.48	4.15	41.1	2.1±1.9	1.38
	17 02.1	In-flight energy calibration								
2	17 16.1	29.1	29.6	54.6	43.5	3.31	3.80	41.1	4.1 1.5	1.16
	17 22.1	In-flight energy calibration								
3	17 29.2	29.1	27.5	49.6	31.1	3.16	3.57	41.1	5.9 1.8	1.03
4	17 39.1	29.1	26.0	45.3	16.9	3.17	3.52	40.2	7.6 2.4	1.01
	17 42.1	In-flight energy calibration								
5	17 45.1	29.1	25.1	42.5	21.1	3.17	3.50	41.4	5.5 2.2	1.00
6	17 53.8	29.1	24.0	38.1	20.3	3.14	3.44	41.4	2.8 2.4	0.97
7	18 01.5	17.1	23.1	34.0	17.7	3.16	3.44	41.1	2.6 2.6	0.97
	18 02.1	In-flight energy calibration								
8	18 07.9	17.1	22.4	30.3	16.5	3.19	3.45	41.1	-0.5 2.7	0.97
9	18 19.5	17.1	21.3	23.2	32.0	3.21	3.45	41.6	3.6 1.9	0.97
	18 22.1	In-flight energy calibration								
10	18 30.4	19.1	20.6	16.0	58.7	3.21	3.42	41.6	4.7 1.3	0.96
11	18 42.1	19.1	20.1	7.8	51.0	3.19	3.40	41.8	5.1 1.4	0.95
	18 42.2	In-flight energy calibration								
12	18 52.1	19.1	20.0	0.7	55.8	3.21	3.41	41.8	6.3 1.3	0.96
	19 02.2	In-flight energy calibration								
	19 42.2	In-flight energy calibration								
13	19 53.7	22.1	24.3	321.3	50.7	3.02	3.32	42.5	6.7 1.4	0.92
	20 02.2	In-flight energy calibration								
14	20 05.0	22.1	25.9	315.9	25.9	3.03	3.36	41.3	6.4 2.1	0.94
15	20 20.2	25.1	28.3	309.4	126.3	2.70	3.07	41.7	7.9 1.1	0.80
	20 22.2	In-flight energy calibration								
16	20 27.3	28.1	29.5	306.8	70.8	2.54	2.91	41.7	4.4 1.4	0.75
17	20 40.1	28.1	31.8	302.4	28.1	2.54	2.99	42.0	11.0 2.0	0.78
	20 42.2	In-flight energy calibration								
18	21 00.4	31.1	35.5	296.3	31.6	2.55	3.14	41.7	7.6 1.9	0.84
	21 02.2	In-flight energy calibration								
19	21 12.1	34.1	37.8	293.3	22.1	2.58	3.26	41.8	11.7 2.2	0.89
	21 22.2	In-flight energy calibration								

*Not corrected for atmospheric absorption or detector response

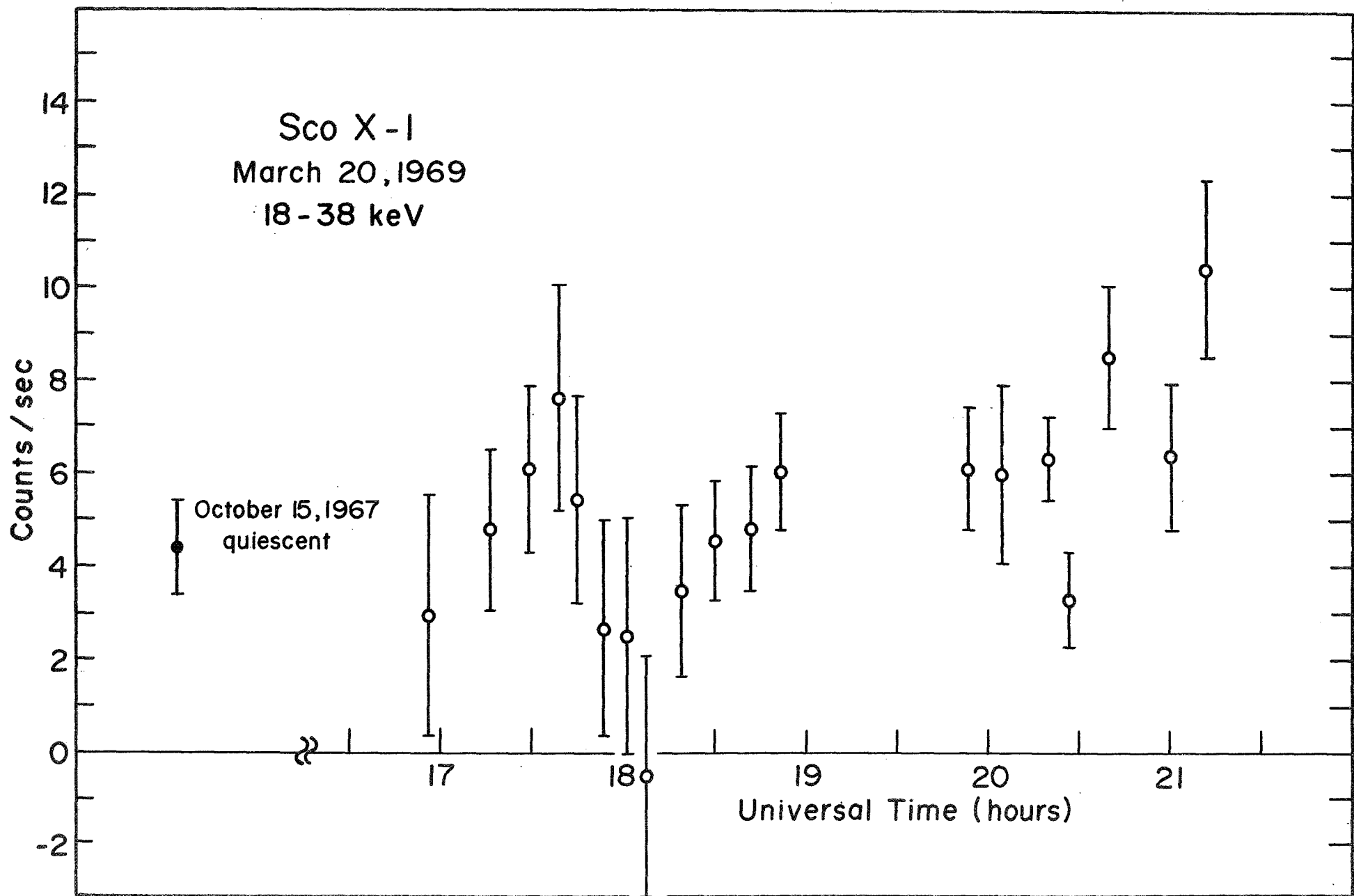


Figure 1

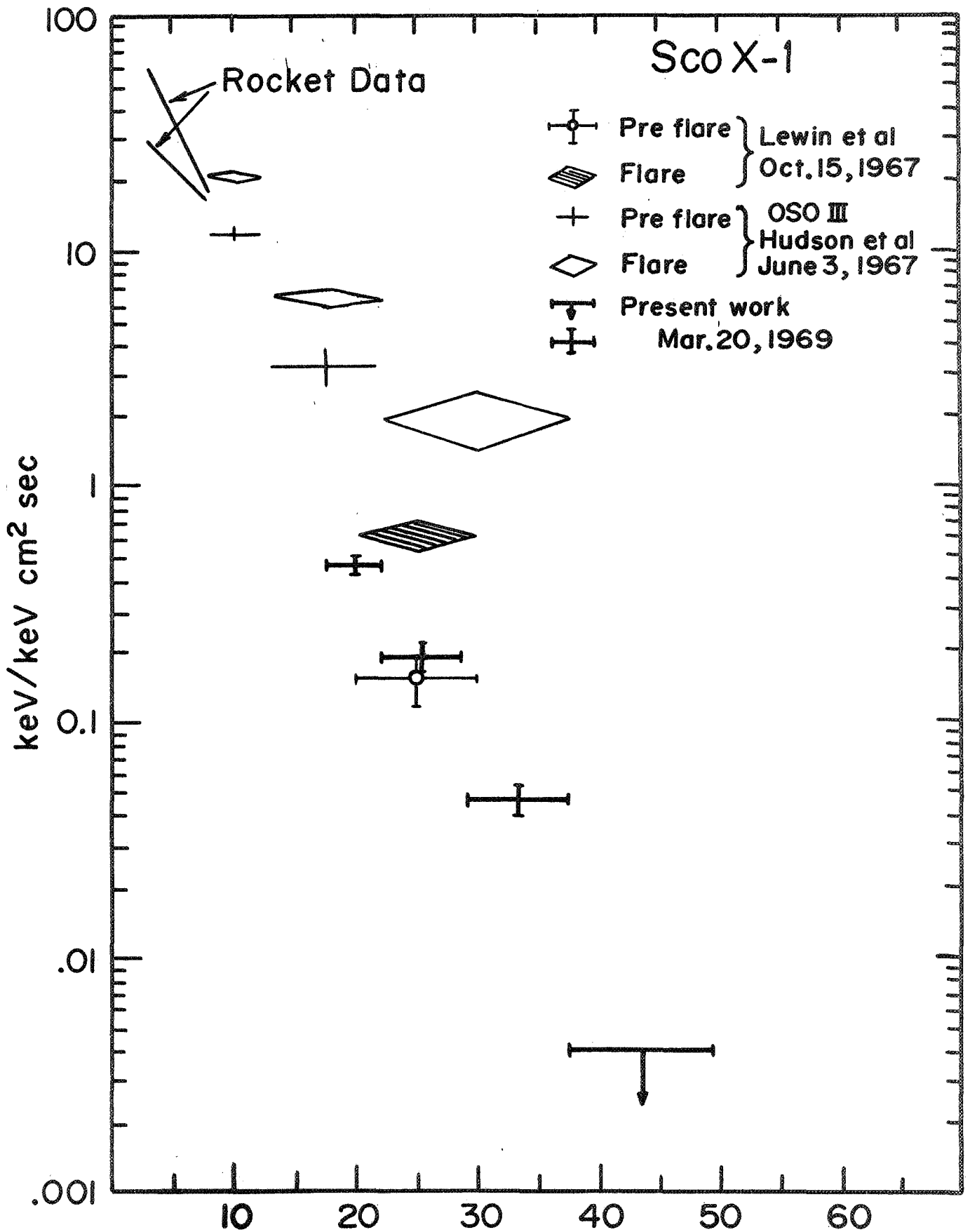


Figure 2